JOURNAL OF Materials CHEMISTRY

Electrochemical quartz crystal microbalance and cyclic voltammetry studies on PbSe electrodeposition mechanisms

Heini Saloniemi,* Marianna Kemell, Mikko Ritala and Markku Leskelä

Department of Chemistry, University of Helsinki, P.O. Box 55, FIN-00014 Helsinki, Finland. E-mail: Heini.Saloniemi@Helsinki.fi

Received 12th August 1999, Accepted 11th November 1999

Electrochemical reactions involved in the electrodeposition of PbSe and the electrochemical behaviour of the related precursors, $HSeO_3^-$ and $Pb(EDTA)^{2-}$, have been studied for the first time by combined electrochemical quartz crystal microbalance and cyclic voltammetry measurements. Formation of PbSe was found to occur by an induced codeposition mechanism *via* a six-electron reduction reaction. $HSeO_3^-$ is reduced by a four-electron reaction but the electrode becomes passivated. The reduction and oxidation of $Pb(EDTA)^{2-}$ occur *via* two-electron mechanisms, on the other hand, during the oxidation adsorption reactions are also observed.

Introduction

PbSe is a narrow band gap photoconductor which is used in IR applications.[1] PbSe thin films have been grown by chemical bath deposition,[2] molecular beam epitaxy,[3] vacuum deposition,[4] successive ionic layer deposition and reaction technique[5] and recently by electrodeposition.[6–8] Mechanistic studies on the electrochemical formation of PbSe have so far been restricted to cyclic voltammetry.[6–8] In this paper we have examined these reactions by combined electrochemical quartz crystal microbalance (EQCM) and cyclic voltammetry measurements. EQCM is a method which has been used to examine, for example, deposition of a metal onto another metal, *i.e.* underpotential deposition mechanisms, redox reactions in self-assembled monolayers[9] and, more recently, electrodeposition of some semiconductors, such as CdTe, CdSe and Cu_xSe_y.[10–13] EQCM gives additional information when combined with cyclic voltammetry; it is a very valuable tool when, for example, cathodic stripping reactions of chalcogenides are studied.

The electrodeposition of PbSe is proposed to occur by an induced codeposition mechanism[6] which means that the deposition of the more noble component, which in the case of PbSe is selenium, induces the deposition of the less noble component, *i.e.* lead. The results in the present paper confirm that the reduction and deposition of lead on selenium occur at more positive potential than on lead itself, and that the electrodeposition of PbSe from $Pb(EDTA)^{2-}$ and $HSeO_3^{2-}$ precursors occurs *via* total six-electron reduction reaction. Also, it was found that the deposition of PbSe occurs at more positive potentials than the reduction of Se^0 to Se^{2-} which suggests that the deposition mechanism involves Se^0 induced reduction of $Pb(EDTA)^{2-}$ rather than precipitation of $Pb(EDTA)^{2-}$ by Se^{2-}.

Experimental

EQCM experiments were carried out in solutions which contained dissolved SeO_2 (Merck), $Pb(CH_3COO)_2$ (Riedel de Haen p.a.), Na_2H_2EDTA (H_4EDTA = ethylenediaminetetraacetic acid) (Riedel de Haen) and $Na(CH_3COO)$ (Merck) in deionized water. The concentration of $Pb(CH_3COO)_2$ was 0.1 M, that of EDTA† *ca.* 0.11 M and that of SeO_2 0.001 M. When selenium was studied without lead, 0.1 M $Na(CH_3COO)$ and 0.1 M EDTA were added to the solutions. According to our previous studies on electrodeposition of PbSe,[6] the experiments were carried out at a pH of *ca.* 3.5. All the experiments were performed at room temperature and the solutions were deaerated with nitrogen prior to the experiments. The solutions were not stirred during the measurement unless otherwise stated.

The electrical equipment consisted of an Autolab PGSTAT20 potentiostat combined with EQCM[14] with an AT-cut 5 MHz quartz crystal. The quartz crystal was covered with a 10 nm Cr adhesion layer and an evaporated 100 nm gold layer which served as a working electrode in the conventional three-electrode cell. The surface area of the working electrode was 0.236 cm^2. A platinum foil was used as a counter electrode and a 3 M KCl/Ag/AgCl electrode was used as a reference electrode. A Fluke PM6680B frequency counter was used to monitor the frequency changes. The voltage scan rate was 10 mV s^{-1}.

According to the Sauerbrey equation the resonant frequency changes Δf of the quartz crystal are correlated with the mass changes Δm [eqn. (1)],

$$\Delta f = -[2{f_0}^2/A(\mu\rho)^{1/2}]\Delta m = -K\Delta m \quad (1)$$

where f_0 is the resonant frequency of the quartz crystal, A is the piezoelectrically active area, μ is the shear modulus of the quartz and ρ its density.[9] However, because the characteristic constant of the crystal, K, is affected by, for example, the crystal roughness and surface area,[15,16] its value is better determined experimentally. Our crystal setup was calibrated by electrodepositing Ag from a solution containing 0.001 M $AgNO_3$ and 0.1 M $HClO_3$ at a potential of −0.2 V *vs.* Ag. Using the Faraday law [eqn. (2)],

$$Q = z\Delta nF \quad (2)$$

where Q is charge consumed during the deposition, obtained by integration of the current, z is the number of electrons, and F is the Faraday constant, and considering that the Ag electrodeposition process is 100% efficient, the mass sensitivity of the quartz crystal was determined from the recorded frequency and charge changes. The value obtained for K was 226 MHz g^{-1} (18.7 ng Hz^{-1} cm^{-2}). This value was used in subsequent calculations.

Electrochemical reactions possibly involved at the substrate surface were examined by plotting the observed frequency

†Here EDTA refers in a general sense to H_nEDTA (n = 1–4) species present in solution.

change (Δf) as a function of the consumed charge (Q). By combining eqns. (1) and (2), and noting that $\Delta m/\Delta n = M$, we have [eqn. (3)],

$$\Delta f = -(KM/Fz)Q \quad (3)$$

where M is the molar mass of the deposit. If the slope of the curve Δf *vs.* Q is assigned as S, then the ratio M/z can be calculated from eqn. (4),

$$M/z = |S|F/K \quad (4)$$

The value of M/z can be exploited in identifying the reaction mechanisms and examining their efficiencies. The slope is positive if a reductive current (negative Q) is accompanied by a frequency decrease (mass increase, deposition) or an oxidative current (positive Q) is accompanied by a frequency increase (mass decrease, dissolution). If no deposition or dissolution occurs in the electrochemical reaction ($M = 0$), the slope is zero. On the other hand, for pure non-electrochemical ($Q = z = 0$) deposition and dissolution reactions, including also adsorption and desorption, M/z is infinite.

Results and discussion

Fig. 1(a), (b) and (c) show cyclic voltammograms at an Au electrode for current, charge and frequency changes, respectively, measured in a solution containing 0.1 M $Pb(EDTA)^{2-}$ at pH 3.5 (solid lines), and in a Pb^{2+} solution without EDTA complexation at the same pH (dotted lines). Lead is reduced according to reaction (5).

$$Pb(EDTA)^{2-}(aq) + 2H^+ + 2e^- \rightleftarrows Pb^0(s) + H_2EDTA^{2-}$$
$$(\text{Theoretical } M/z = 207.2/2 = 103.6 \text{ g mol}^{-1}) \quad (5)$$

The complexing agent EDTA moves the reduction potential of Pb to a much more negative value and also differences in the oxidation behaviour are observed. During the reverse scan several oxidation waves are seen only in the presence of the complexing agent [Fig. 1(a)]. The first oxidation peak could be due to oxidation of Pb^0 which is immediately complexed by EDTA since the oxidation occurs at more negative potential than where Pb^0 oxidises in the absence of EDTA. The second wave could be due to oxidation of Pb^0 but without the immediate complexation with EDTA which could be delayed if the surface concentration of EDTA was diminished.

Formation of a Pb–Au alloy could explain one of the separate oxidation waves; indeed, signs of this alloy were observed in an X-ray diffraction (XRD) measurement performed after the negative scan. However, the XRD peaks corresponding to the Pb–Au alloy were rather weak and largely overlapped with the peaks which corresponded to Au or Pb themselves. Several oxidation waves have been observed also in the study on the underpotential deposition (UPD) of Pb on gold.[17] In this instance the different oxidation waves were ascribed to the different crystal faces of the substrate. However, the frequency change for the deposition of one monolayer of Pb^0 would be only be *ca.* 6 Hz[17] and thus in our case the amount of Pb^0 deposited during the cyclic voltammogram was much more. Also in the oxidation of Pb^0 on the top of SnO_2 at pH 9[18] several waves were observed which excludes Pb–Au alloy formation as the only reason for the multiple oxidation waves. On the other hand, the reoxidation of the previously reduced tin in the SnO_2 substrate may have also been involved.

A notable increase in the mass was observed during the oxidation in the presence of EDTA at *ca.* −0.30 V *vs.* Ag/AgCl [Fig. 1(c)]. When the cyclic voltammograms were measured between different potentials it was found that the more negative the end potential, the larger the mass increase during the reduction of lead but at the same time also the mass increase during the oxidation became larger. Thus, it is

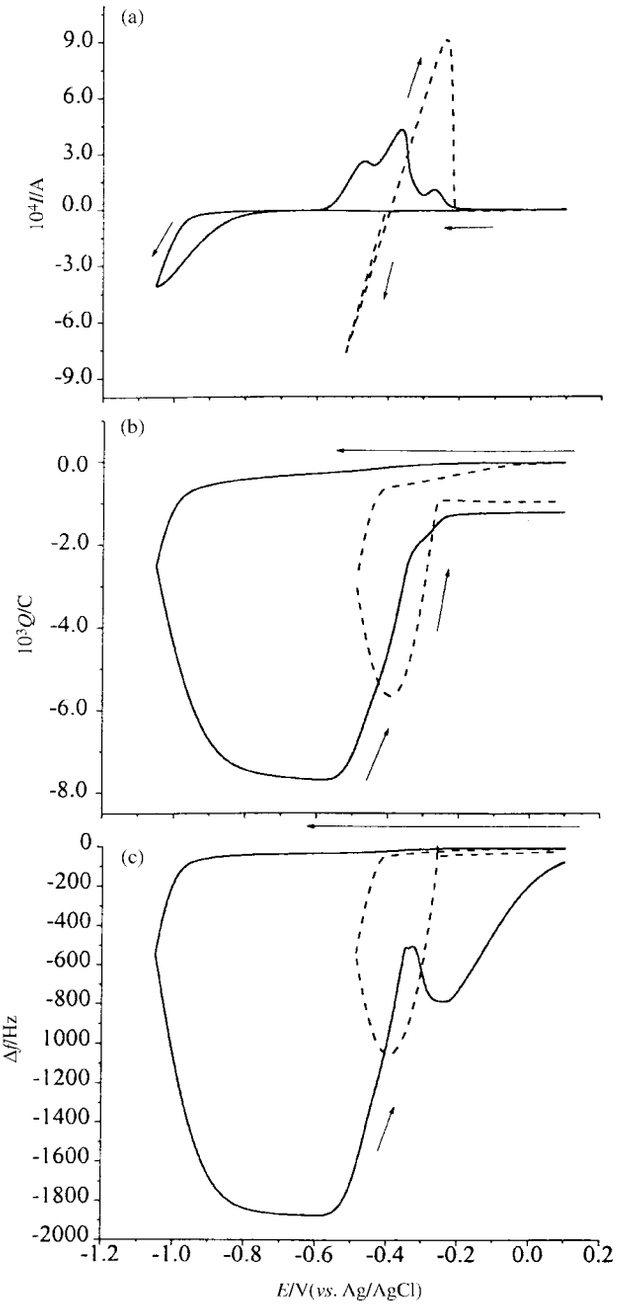

Fig. 1 Cyclic voltammograms on an Au electrode for current (a), charge (b) and frequency (c) changes measured in a solution containing 0.1 M $Pb(EDTA)^{2-}$ at pH 3.5 (solid lines), and in a Pb^{2+} solution without EDTA complexation at the same pH (dotted lines).

proposed that the oxidising lead reacts with some species in the solution, most probably free EDTA, while still on the surface of the substrate. At a potential of −0.28 V *vs.* Ag/AgCl, the mass starts to decrease again, but this decrease continues even when the current has stopped to flow, which is most probably due to a rather slow desorption of the soluble species from the substrate surface. For comparison, EQCM and voltammetric measurements were also carried out in a stirred solution where the transportation is accelerated (Fig. 2). It can be seen that there is no mass increase during the oxidation and the frequency returns close to zero as soon as the current stops to flow. Clearly, the slow diffusion of the desorbing species away from the surface is responsible for the observed mass increase during the oxidation as well as one of the multiple oxidation waves in the non-stirred solution.

Fig. 3 shows the Δf *vs.* Q curve as evaluated from Fig. 1(b) and (c). The M/z value between the potentials of −0.95 and

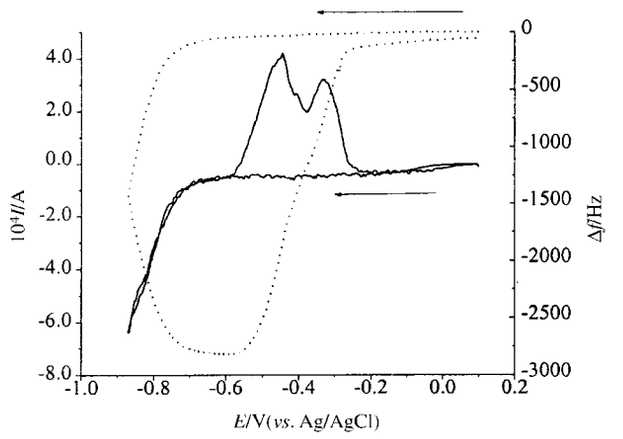

Fig. 2 Cyclic voltammogram on an Au electrode (solid line) and corresponding frequency curve (dotted line) measured in a stirred solution containing 0.1 M $Pb(EDTA)^{2-}$ at pH 3.5.

−1.0 V *vs.* Ag/AgCl calculated from the slope of this plot is 103.3 g mol^{-1} which is very close to the *M*/*z* value corresponding to the two-electron reduction of lead, *i.e.* 103.6 g mol^{-1} [reaction (5)]. Between the potentials of −1.00 and −1.05 V and during the reduction in the reversed scan from −1.05 to −0.85 V *vs.* Ag/AgCl, the *M*/*z* values are larger, 112.6 and 113.2 g mol^{-1}, respectively. Since the efficiency of the reduction cannot exceed 100%, the large *M*/*z* values during the reduction seem to be caused by the adsorption and incorporation of *e.g.* EDTA during the deposition of lead. This could arise from the porous morphology of the depositing Pb film. The reduction of H^+, which most probably also occurs at such negative potentials, would diminish the *M*/*z* value. On the other hand, since Δf returns to its original level at the end of the scan while *Q* does not, it appears that some H^+ reduction occurred. At the beginning of the oxidation, between the potentials of −0.5 and −0.4 V *vs.* Ag/AgCl, EDTA appears to desorb together with the oxidising lead since the *M*/*z* value is high, 122.8 g mol^{-1}. The *M*/*z* value closest to the two-electron oxidation reaction was reached between the potentials of −0.4 and −0.32 V *vs.* Ag/AgCl (108.4 g mol^{-1}). When the mass increased during the oxidation between the potentials of −0.32 and −0.28 V *vs.* Ag/AgCl, the *M*/*z* value was large, 360.7 g mol^{-1}, which also reflects adsorption effects.

The *M*/*z* values obtained for the reduction of uncomplexed Pb^{2+} solution were 104.1 g mol^{-1} between potentials of −0.42 and −0.46 V *vs.* Ag/AgCl, and 81.9 g mol^{-1} between potentials of −0.46 and −0.5 V *vs.* Ag/AgCl. For the oxidation during the reversed scan 78.9 g mol^{-1} (−0.42 to −0.28 V) and

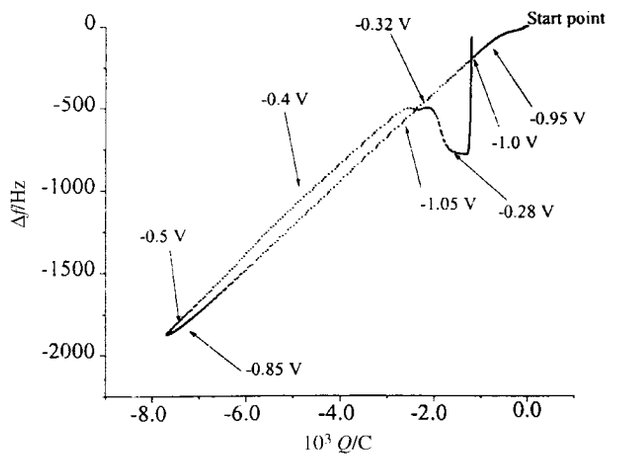

Fig. 3 The Δf *vs.* *Q* curve plotted from the cyclic voltammogram in Fig. 1 in a solution containing 0.1 M $Pb(EDTA)^{2-}$ at pH 3.5.

102.3 g mol^{-1} (−0.28 to −0.26 V *vs.* Ag/AgCl) were obtained. Thus during the reduction of Pb^{2+} the *M*/*z* value is closest to the theoretical value at the very beginning of the reduction and during the end of the oxidation.

In the case of selenium, which is in the form of $HSeO_3^{2-}$ at pH 3.5,[19] the preliminary experiments revealed that the oxidation of Se during the reversed scan started at a potential of 0.5 V *vs.* Ag/AgCl but it was not studied further since the Au/Cr substrate started to oxidise before selenium was fully oxidized. In order to imitate the deposition conditions of PbSe, the measurements were performed in two 0.001 M $HSeO_3^{2-}$ solutions containing either only 0.1 M $Na(CH_3COO)$ (Fig. 4 dotted line) or both 0.1 M $Na(CH_3COO)$ and 0.1 M EDTA (Fig. 4 solid line) on the Au surface. Since Se^0 reduces further to H_2Se [eqn. (6)] complicating the interpretation of the $HSeO_3^-$ measurements, this reaction was examined first by the measurement made with a previously deposited selenium film in a solution which contained 0.1 M $Na(CH_3COO)$ and no $HSeO_3^-$ (Fig. 5).

$$Se^0(s) + 2e^- + 2H^+ \rightleftharpoons H_2Se\,(aq)$$
$$(M/z = 78.96/2 = 39.5\ g\ mol^{-1}) \qquad (6)$$

The reduction reaction which leads to the mass decrease begins at a potential of −0.45 V *vs.* Ag/AgCl. The corresponding *M*/*z* value is 34.3 g mol^{-1} which refers to reaction (6). When the measurement was made in a solution also containing 0.1 M EDTA the stripping reaction was found to begin at the same potential.

From Fig. 4 it is seen in both solutions that on an Au electrode at potentials more positive than −0.4 V *vs.* Ag/AgCl there is small current with a small increase in the mass (frequency change of *ca.* 10–20 Hz). This so-called predeposition wave was observed only during the very first cycle. It is proposed that it is due to a phenomenon similar to the metal UPD process where the first monolayer is deposited before the bulk deposition. A difference, however, is that under these conditions the reduction of selenium has a very large overpotential, which the metals do not have and are deposited at underpotentials with respect to their equilibrium potentials. If this Se monolayer is not dissolved before the next cycle, such predeposition current and mass changes are not observed subsequently. The same type of predeposition has also been found in earlier studies on tellurium and selenium.[20,21] At a potential of −0.4 V *vs.* Ag/AgCl a large reduction wave is seen to arise. Between potentials of −0.5 and −0.7 V *vs.* Ag/AgCl, *M*/*z* is 19.9 g mol^{-1} [Fig. 6(a)] corresponding to the four-electron reduction reaction (7) though the same *M*/*z* value is obtained if reaction (8), or the successive reactions (7) and (6), are quantitatively followed by the chemical reaction (9).

$$HSeO_3^-(aq) + 5H^+ + 4e^- \rightleftharpoons Se^0 + 3H_2O$$
$$(M/z = 78.96/4 = 19.74\ g\ mol^{-1}) \qquad (7)$$

$$HSeO_3^-(aq) + 7H^+(aq) + 6e^- \rightleftharpoons H_2Se\,(aq) + 3H_2O$$
$$(M/z = 0\ g\ mol^{-1}) \qquad (8)$$

$$2H_2Se(aq) + H^+ + HSeO_3^-(aq) \rightleftharpoons 3Se^0\,(s) + 3H_2O \qquad (9)$$

If reaction (9) is fast enough, the overall reaction will be a four-electron reduction reaction.[22] H_2Se is most probably involved in the formation of Se^0 since it is formed at this potential range (Fig. 5). At a potential of *ca.* −0.7 V *vs.* Ag/AgCl, the *M*/*z* value decreases to from 9.9 to 3.1 g mol^{-1} as the reduction of hydrogen begins and possibly reaction (8) occurs simultaneously. In the solution containing EDTA the current starts to increase at somewhat more positive potential than in the solution without EDTA (Fig. 4).

During the second scan, only at the very beginning of the

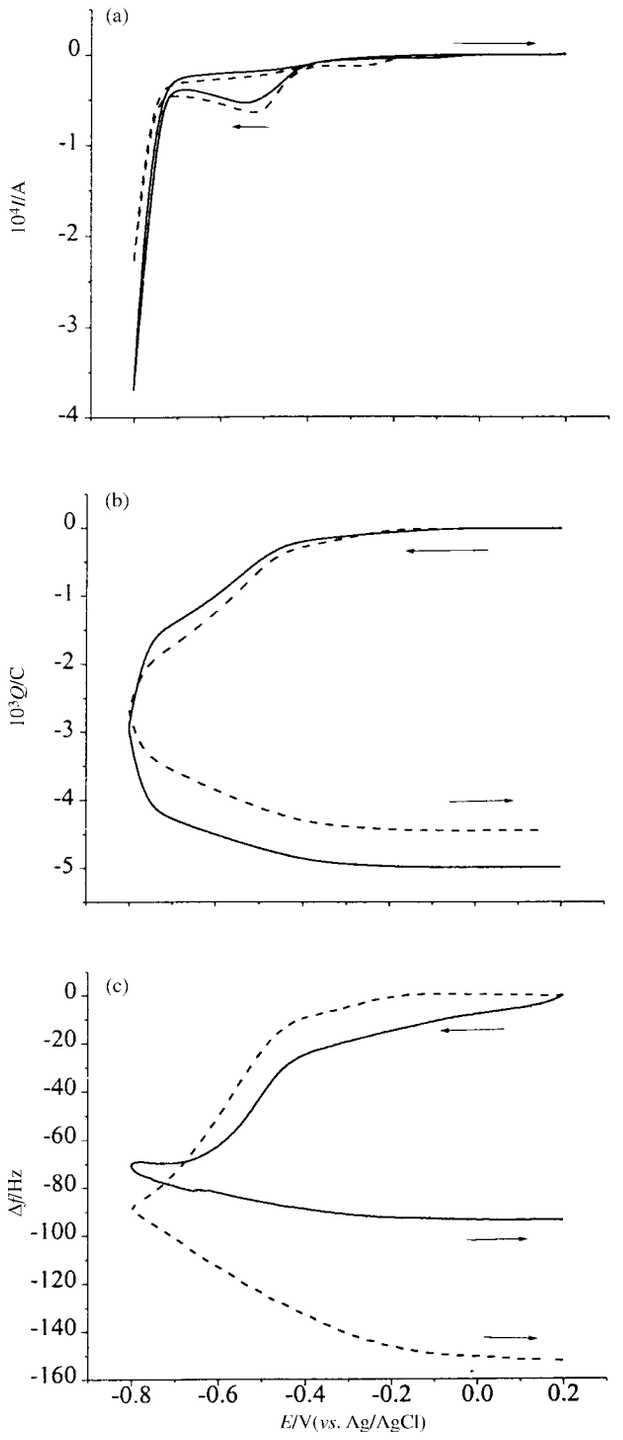

Fig. 4 Cyclic voltammograms on an Au electrode for current (a), charge (b) and frequency (c) changes measured in a solution containing 0.001 M $HSeO_3^-$ and 0.1 M $Na(CH_3COO)$ (dotted lines), and in a 0.001 M $HSeO_3^-$ solution containing 0.1 M $Na(CH_3COO)$ and 0.1 M EDTA.

reduction wave, between potentials of −0.37 and −0.47 V *vs.* Ag/AgCl, the *M*/*z* value (17.3 g mol^{-1}) is fairly close to the four-electron reduction reaction value but in the potential range −0.47 to −0.65 V *vs.* Ag/AgCl the *M*/*z* value is lower at 13.5–14.9 g mol^{-1} [Fig. 6(b)] probably due to simultaneous reactions (6) and (8) in addition to reaction (7). Also passivation of the surface was observed since both charge and frequency changes were smaller during the second scan than during the first scan. Passivation appears to be more efficient in the solution containing EDTA since the deposition of Se has been suppressed already during the reversed scan of the first cycle (Fig. 4).

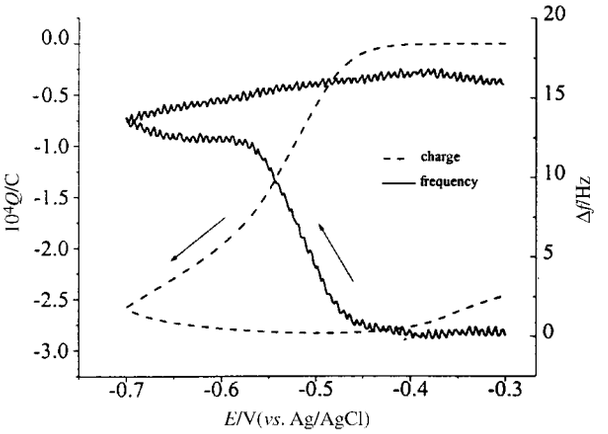

Fig. 5 The frequency (solid line) and charge (dashed line) curves measured in the solution containing 0.1 M $Na(CH_3COO)$ with Se film deposited on a gold electrode.

Fig. 7 shows the *M*/*z* values obtained when selenium was deposited at different constant potentials in solutions which contained either only $Na(CH_3COO)$ or both $Na(CH_3COO)$ and EDTA on the gold surface. When selenium was deposited at a constant potential of −0.3 V *vs.* Ag/AgCl, the *M*/*z* values were 19.1 and 19.9 g mol^{-1}, respectively, but the deposition stopped after 10–20 Hz. At a potential of −0.4 V *vs.* Ag/AgCl in both solutions the *M*/*z* values of 20.6 and 19.9 g mol^{-1} were very close to the theoretical value of the four-electron reduction reaction (7). At a more negative potential of −0.65 V *vs.* Ag/AgCl, the deposition was suppressed; in the solution containing no EDTA, *M*/*z* was 24.2 g mol^{-1} for the first 10 s and then fell to 16.2 g mol^{-1}, while in the solution containing EDTA the

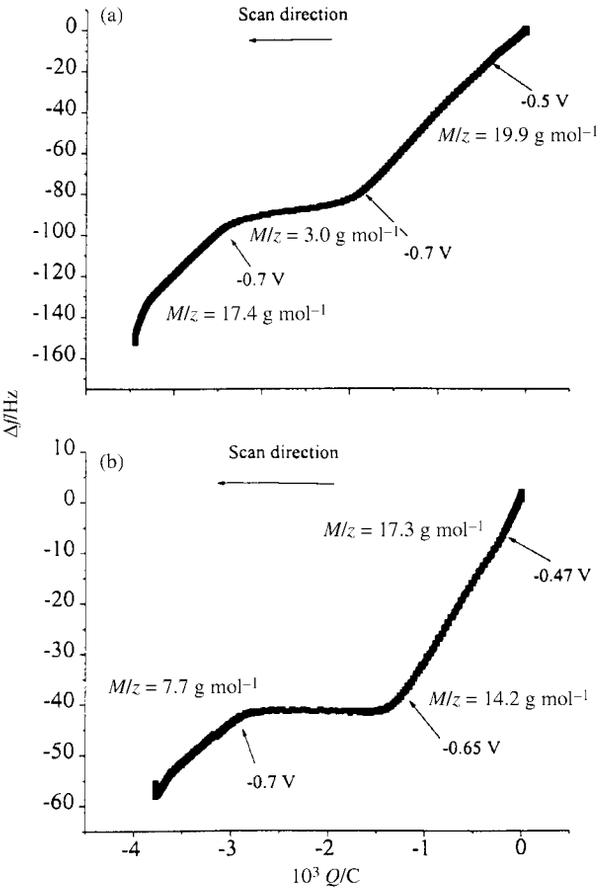

Fig. 6 (a) The Δf *vs.* Q curve plotted from the cyclic voltammogram in Fig. 4 in a solution containing 0.001 M $HSeO_3^-$ and 0.1 M $Na(CH_3COO)$. (a) The first scan and (b) the second scan.

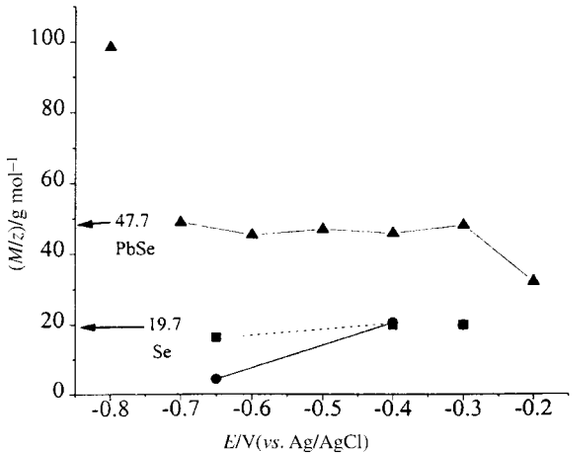

Fig. 7 The *M*/*z* values calculated from the different constant potential measurements in the solutions containing 0.001 M $HSeO_3^-$ and 0.1 M $Na(CH_3COO)$ (■), 0.001 M $HSeO_3^-$, 0.1 M $Na(CH_3COO)$ and 0.1 M EDTA (●) and $Pb(EDTA)^{2-}$ and $HSeO_3^-$ (▲). The depositions were made on an Au surface. The theoretical *M*/*z* values for the six-electron reduction reaction for formation of PbSe [reaction (10)] and the four-electron reduction reaction for Se [reaction (7)] are indicated by the arrows.

M/*z* value for the first 10 s was 18.7 g mol^{-1} and then decreased to 4.3 g mol^{-1}. This can be explained by the fact that at this potential the formation of H_2Se is also involved in the reactions leading not only to the chemical reaction (8) but also to stripping of the Se^0 film. Also the reduction of hydrogen diminishes the *M*/*z* value.

From the results above, it can be concluded that deposition of Se occurs *via* a four-electron reduction reaction between potentials of −0.4 and −0.7 V *vs.* Ag/AgCl but that also other simultaneous reactions exist. At a potential of −0.45 V *vs.* Ag/AgCl, Se^0 is reduced further to H_2Se and at a potential of *ca.* −0.7 V *vs.* Ag/AgCl hydrogen is evolved.

Fig. 8(a), (b) and (c) show the cyclic voltammograms for current, charge and frequency, respectively, measured in a solution containing both $Pb(EDTA)^{2-}$ and $HSeO_3^{2-}$ precursors on a bare Au electrode (solid line) and on a PbSe film deposited previously at a potential of −0.7 V *vs.* Ag/AgCl for 60 s (dotted line).The corresponding Δf *vs.* *Q* curve is shown in Fig. 9.

The *M*/*z* value of 46.9 g mol^{-1} between the potentials −0.3 and −0.7 V *vs.* Ag/AgCl corresponds well to the six-electron reaction (10).

$$HSeO_3^-(aq) + Pb(EDTA)^{2-}(aq) + 7H^+ + 6e^- \rightleftharpoons PbSe\ (s) + 3H_2O + H_2EDTA^{2-}\ (aq) \quad (M/z = 28/6 = 47.69\ g\ mol^{-1}) \qquad (10)$$

Another possibility for the six-electron reaction would be reaction (8) followed by reaction (11).

$$Pb(EDTA)^{2-}(aq) + H_2Se(aq) \rightleftarrows PbSe(s) + H_2EDTA^{2-}(aq) \qquad (11)$$

On the other hand, reaction (11) does not occur if $HSeO_3^-$ is not reduced to H_2Se but only to Se^0 which is most probable at potentials more positive than −0.45 V *vs.* Ag/AgCl (*cf.* Fig. 5). Reaction (11) could in principle be a simultaneous reaction pathway at more negative potentials (in the range −0.45 to −0.70 V *vs.* Ag/AgCl), since the formation of H_2Se was observed in this potential range (Fig. 5).

At potentials more negative than −0.7 V *vs.* Ag/AgCl the *M*/*z* value increases to 88.8 g mol^{-1}, which implies that the reduction of $Pb(EDTA)^{2-}$ to Pb^0 [reaction (5)] starts to compete with the formation of PbSe (Fig. 9). The reduction

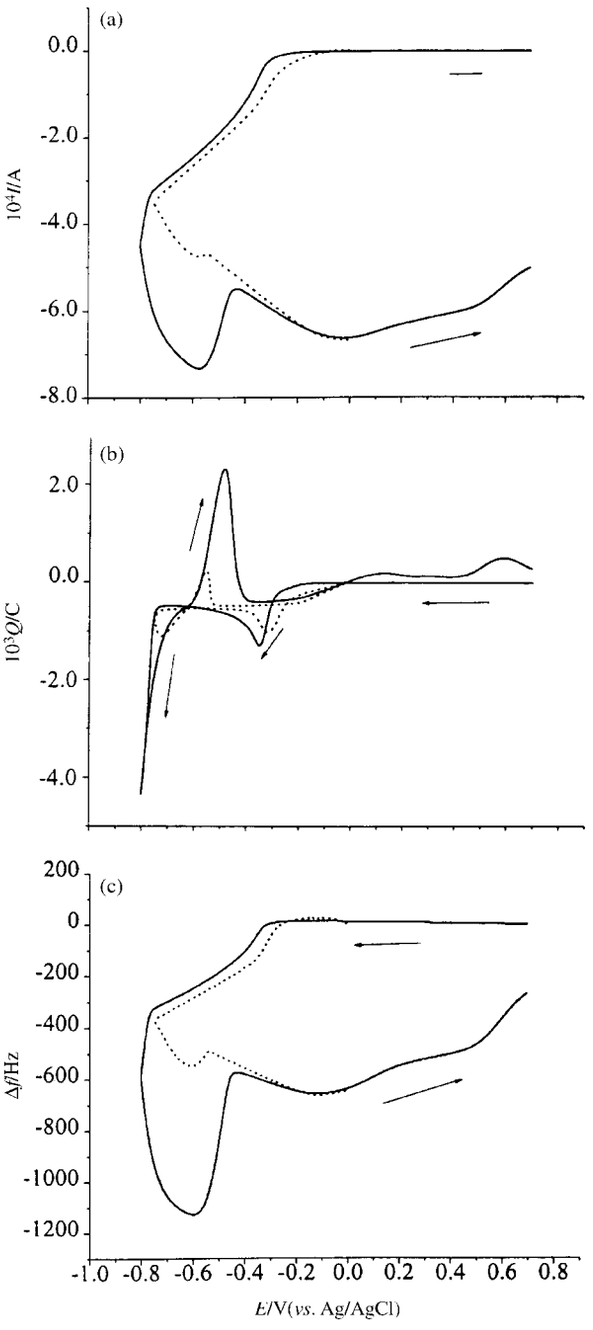

Fig. 8 Cyclic voltammograms for current (a), charge (b) and frequency (c) measured in a solution containing 0.1 M $Pb(EDTA)^{2-}$ and 0.1 M $HSeO_3^{2-}$ measured with Au (solid line) and PbSe film deposited at −0.7 V *vs.* Ag/AgCl for 60 s (dotted line).

of Pb^{2+} to Pb^0 has moved to a more positive potential, as compared with Fig. 1, so the deposition of Pb is more favourable on the PbSe surface than on the bare Au surface. During the reversed scan, the first oxidation wave is observed between potentials −0.55 and −0.45 V *vs.* Ag/AgCl [Fig. 8(a)], the *M*/*z* value being 122.5 g mol^{-1}. This wave arises from the oxidation of metallic lead and possibly simultaneous desorption of EDTA since a similar oxidation wave and *M*/*z* value were observed when the voltammogram was measured without selenium (Fig. 1). Between potentials of −0.45 and −0.20 V *vs.* Ag/AgCl the reduction reaction continues but the *M*/*z* value is reduced to 38.0 g mol^{-1} owing either to inefficient formation of PbSe or deposition of an Se rich film. A PbSe film starts to oxidise at a potential of 0.0 V *vs.* Ag/AgCl and between potentials of 0.0 and 0.1 V *vs.* Ag/AgCl the *M*/*z* value is 143.8 g mol^{-1}. This value corresponds

to the two-electron oxidation of PbSe which can occur if only Pb is oxidised and the resulting Se^0 is detached from the surface as a consequence of the reduction of the underlying PbSe [reaction (12)].

$$PbSe(s) + H_2EDTA^{2-}(aq) \rightleftarrows Pb(EDTA)^{2-}(aq) + Se^0(\text{colloid, aq}) + 2e^- + 2H^+ \quad (M/z = 286.16/2 = 143.1 \text{ g mol}^{-1}) \qquad (12)$$

The M/z value between potentials of 0.1 and 0.2 V *vs.* Ag/AgCl is 103.6 g mol^{-1}, which is the same as for the oxidation of Pb^0. At more positive potentials of 0.25–0.45 and 0.5–0.7 V *vs.* Ag/AgCl the M/z values were 71.6 and 101.5 g mol^{-1}, respectively, which do not correspond to the theoretical values for the oxidation of Pb, Se or PbSe probably owing to the fact that several oxidation reactions occur simultaneously. Also oxidation of the substrate is possible between potentials of 0.5 and 0.7 V *vs.* Ag/AgCl.

When the measurements were made with a previously deposited PbSe film the deposition of PbSe starts at a slightly more positive potential than with a bare Au substrate. Also the deposition of elemental lead seems to be greatly suppressed on PbSe as compared to Au but this is due to the different turning points in the potential scans. Otherwise the changes in both current and charge are quite similar.

In order to further study the induced codeposition of lead, a cyclic voltammogram was also measured with a previously deposited selenium film in a solution containing only 0.1 M $Pb(EDTA)^{2-}$ starting from a potential of −0.1 V *vs.* Ag/AgCl (Fig. 10). The current starts to flow and the mass increases at −0.3 V *vs.* Ag/AgCl, *i.e.* at much more positive potential than for the reduction of lead on Au (Fig. 1). The M/z value between potentials of −0.3 and −0.7 V *vs.* Ag/AgCl was 99.7 g mol^{-1} which is close to the M/z value of the reduction of lead [reaction (5)]. During the reversed scan, which was measured up to a potential of 0.6 V *vs.* Ag/AgCl, oxidation starts at 0.0 V which is the same potential where the second oxidation wave, *i.e.* that attributed to PbSe, was observed (Fig. 8). The M/z value during the oxidation is 134.8 g mol^{-1} which corresponds quite well to a two-electron oxidation of PbSe [reaction (13)]. In addition, since the oxidation wave of Pb^0 was not observed between the potentials of −0.6 and −0.2 V *vs.* Ag/AgCl (*cf.* Fig. 1), it is concluded that all the lead deposited formed PbSe. These results confirm that Se^0 induces the reduction of Pb^{2+} leading to the formation of PbSe.

In the constant potential growth experiments, PbSe was deposited at potentials of −0.2 and −0.8 V *vs.* Ag/AgCl for 1 min and the M/z values evaluated from these experiments are presented in Fig. 7; these results support the voltammetric

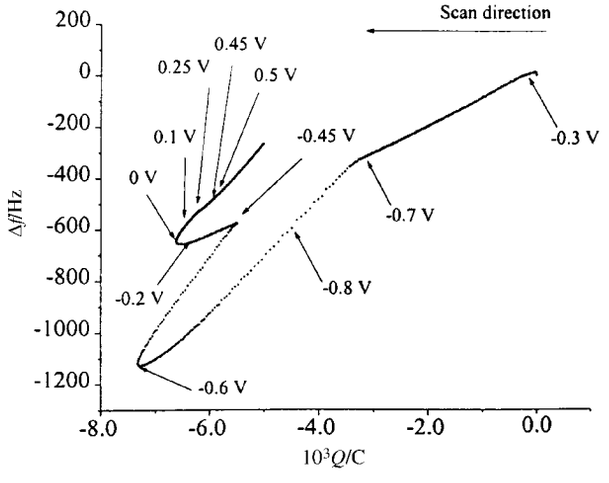

Fig. 9 The Δf *vs.* Q curve measured in the solution containing 0.1 M $Pb(EDTA)^{2-}$ and 0.001 M $HSeO_3^{2-}$ at pH 3.5.

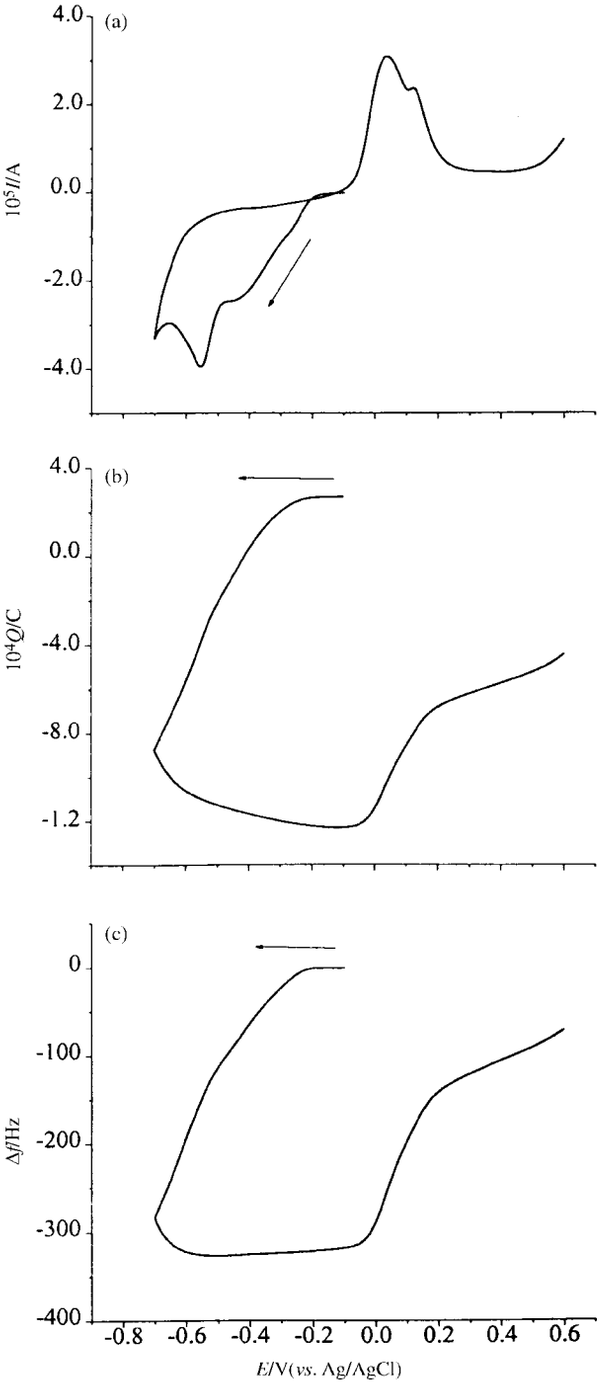

Fig. 10 Cyclic voltammograms for current (a), charge (b) and frequency (c) measured in a solution containing 0.1 M $Pb(EDTA)^{2-}$ with Se film deposited at a potential of −0.4 V *vs.* Ag/AgCl for 180 s.

results. At a potential of −0.2 V *vs.* Ag/AgCl, Se rich PbSe is deposited, while between the potentials of −0.3 and −0.7 V *vs.* Ag/AgCl six-electron formation of PbSe occurs, and at −0.8 V *vs.* Ag/AgCl the deposition of a lead rich film is observed. In our earlier study where PbSe films were grown on an SnO_2 surface, the potential range of stoichiometric PbSe films, as analysed by energy dispersive X-ray spectrometry and Rutherford backscattering spectrometry, was −0.4 to −0.75 V *vs.* SCE[6] which correlates well with the present EQCM results.

Conclusions

EQCM measurements complete the cyclic voltammetry studies on the electrodeposition mechanism of thin films of PbSe. The

deposition of PbSe occurs by induced codeposition *via* an efficient six-electron reduction reaction, whereas the oxidation of PbSe is *via* a two-electron reaction. The reduction of $Pb(EDTA)^{2-}$ to elemental lead occurs *via* a two-electron reaction with simultaneous adsorption reactions. Selenium deposits *via* a four-electron reaction also involving the formation of H_2Se.

Acknowledgements

This work is partly supported by the National Technology Agency (TEKES), Academy of Finland and the special funding of the University of Helsinki.

References

1 T. H. Johnson, *Proc. SPIE, Int. Soc. Opt. Eng.*, 1984, **443**, 60.
2 S. Gorer, A. Albu-Yaron and G. Hodes, *Chem. Mater.*, 1995, **7**, 1243.
3 H. Zogg, C. Maissen, J. Masek, T. Hoshino, S. Blunier and A. N. Tiwari, *Semicond. Sci. Technol.*, 1991, **6**, C36.
4 V. Damoradara Das and K. Seetharama Bhat, *J. Mater. Sci.*, 1990, **1**, 169.
5 T. Kanniainen, S. Lindroos, J. Ihanus and M. Leskelä, *J. Mater. Chem.*, 1996, **6**, 983.
6 H. Saloniemi, T. Kanniainen, M. Ritala, M. Leskelä and R. Lappalainen, *J. Mater. Chem.*, 1998, **8**, 651.
7 A. N. Molin and A. I. Dikusar, *Thin Solid Films*, 1995, **265**, 3.
8 E. A. Streltsov, N. P. Osipovich, L. S. Ivanshkevich, A. S. Lyakhov and V. V. Sviridov, *Electochim. Acta*, 1998, **43**, 869.
9 D. Buttry and M. Ward, *Chem. Rev.*, 1992, **92**, 1355.
10 C. Wei, N. Myung and K. Rajeshwar, *J. Electroanal. Chem.*, 1993, **347**, 223.
11 J. G. N. Matias, J. F. Juliao, C. M. Soares and A. Gorenstein, *J. Electroanal. Chem.*, 1997, **431**, 163.
12 A. Marlot and J. Vedel, *J. Electrochem. Soc.*, 1999, **146**, 177.
13 C. Wei, C. S. C. Bose and K. Rajeshwar, *J. Electroanal. Chem.*, 1992, **327**, 331.
14 W. Koh, W. Kutner, M. T. Jones and K. M. Kadish, *Electroanalysis*, 1993, **5**, 209.
15 S. Bruckenstein and M. Shay, *Electrochim. Acta*, 1985, **30**, 1295.
16 C. Gabrelli, M. Keddam and R. Torresi, *J. Electrochem. Soc.*, 1991, **138**, 2657.
17 M. R. Deakin and O. Melroy, *J. Electroanal. Chem.*, 1988, **239**, 321.
18 H. Saloniemi, T. Kanniainen, M. Ritala and M. Leskelä, *Thin Solid Films*, 1998, **326**, 78.
19 C. Baes and R. Messner, *The Hydrolysis of Cations*, John Wiley & Sons, New York, 1976, p. 348.
20 T. A. Sorenson, T. E. Lister, B. M. Huang and J. L. Stickney, *J. Electrochem. Soc.*, 1999, **146**, 1019.
21 E. Mori, C. K. Baker, J. R. Reynolds and K. Rajeshwar, *J. Electroanal. Chem.*, 1988, **252**, 441.
22 M. Skyllas Kazacos and B. Miller, *J. Electrochem. Soc.*, 1980, **127**, 869.

Paper a906557a